GEOLOGICAL OUTCROP MODELLING AND INTERPRETATION USING GROUND BASED HYPERSPECTRAL AND LASER SCANNING DATA FUSION

T. H. Kurz[a, b,*], S. J. Buckley[a], J. A. Howell[a], D. Schneider[c]

[a]Centre for Integrated Petroleum Research, University of Bergen, Postboks 7800, N-5020 Bergen, Norway - tobias.kurz@cipr.uib.no, simon.buckley@cipr.uib.no, john.howell@cipr.uib.no
[b]Department of Earth Science, University of Bergen, Postboks 7800, N-5020 Bergen, Norway
[c]Institute of Photogrammetry and Remote Sensing, Technische Universität Dresden, D-01062 Dresden, Germany - danilo.schneider@tu-dresden.de

Commission VIII/12

KEY WORDS: Laser, Integration, Lidar, Close Range, Hyper spectral, Mapping, Geology

ABSTRACT

Recent developments in the utilisation of close range laser scanning (lidar) in geology have seen the increased use of virtual outcrop data. The remote mapping of rock properties within the virtual outcrop remains, however, a challenge. This study aims to develop methods for combining and utilising data from close range lidar and ground based hyperspectral scanning. The workflow for using such data is presented for a case study of a dolomite and limestone quarry in the Peak District, UK. Multiple hyperspectral and lidar scans were acquired simultaneously to gain both spectral and geometric data. Different image processing algorithms were utilised to extract and map geological features from the spectral images, resulting in thematic images. To register the spectral images to the lidar coordinate system, the scanning sensor was modelled using cylindrical imaging geometry, as the central perspective projection is unsuitable for a rotating array. Bundle adjustment permitted the hyperspectral image orientation and position to be calculated, allowing the integration to be completed. The classified and registered imagery was used to colour the lidar point cloud, and this was superimposed with a textured 3D model of the outcrop, allowing interpretation and validation. The preliminary results showed areas of limestone and low dolomitization in the upper part of the quarry thought to have been only dolomite. This combination of geometrically accurate lidar data and spectral mapping of lithology has significant implications for the improved collection of geological data.

1. INTRODUCTION

Geological outcrops (locations with well exposed and uncovered rocks) have long been used as analogues for subsurface hydrocarbon reservoirs. In the subsurface, data comes from direct measurement of the reservoir in a limited number of well bores which are often kilometres apart, and seismic imaging which has a vertical resolution of tens of metres. The geological heterogeneities that control the flow of fluids and the recovery of hydrocarbons are not typically measurable or able to be mapped. Consequently analogous geological outcrops are used to provide input for geological models. In recent years there have been numerous advances in the collection and application of spatial constrained outcrop data (see for example McCaffrey et al., 2005). A key development has been the application of close range laser scanning to the 3D mapping of geological outcrops. Lidar scanning allows an extremely accurate representation of the geology with high spatial resolution and geometrical accuracy. Once captured in digital form, the data can be used to generate virtual outcrops as a means for studying geometries and extracting meaningful spatial information (e.g. Bellian et al., 2005; Buckley et al., 2006; Sagy et al., 2007; Buckley et al., 2008). This spatial data can be loaded into geocellular modelling systems and used as a means of understanding geological architectures and their effects on the behaviour of hydrocarbon reservoirs and aquifers (Enge et al., 2007).

Most modern lidar systems used in geology are linked to a high resolution digital camera, which allows the lidar point cloud to be coloured and provides texture for mapping onto surfaces created from the scanned point set. Texture mapping the digital surface provides the most easily interpretable dataset, as using the point cloud alone cannot provide the level of detail required when making close-up examinations, even with extremely dense point spacing. The virtual outcrop is then used by the geologist to map and interpret geological features. To date, most of the interpretation is carried out manually (Buckley et al., 2008), and the semi-automatic extraction of features such as mineralogy, rock type, faults and bedding surfaces from the lidar data and virtual outcrops remains a major challenge using only the lidar geometry and visible wavelength images. This paper reports on research that aims to develop methods integrating ground based hyperspectral data into the current workflow, ultimately leading to the remote mapping of lithology and petrophysical properties in virtual outcrops.

2. MOTIVATION

Hyperspectral imaging has already been proven successful in the field of geology for the regional mapping of rock types and mineral prospecting using airborne and spaceborne sensors (e.g. Windeler and Lyon, 1991; Bowen et al., 2007). Bowen et al. (2007) demonstrates the use of airborne

* Corresponding author.

hyperspectral images (HyMap) to map the diagenetic heterogeneities and fluid-flow pathways in a sandstone environment with favourable reservoir properties. This work points out the potential of spectral scanning for reservoir analogue modelling. However, the outcrops studied in the current research are typically near-vertical cliff sections and quarries, making the use of airborne or spaceborne data unsuitable. An additional factor excluding the use of airborne data is related to the scale of features studied. Using aerial data, large areas can easily be captured, allowing regional interpretations to be made. For near-vertical outcrops, features may be much smaller, requiring the instrumentation to be positioned at close range. A non-contact method is also desirable: outcrops are often high and steep, and it is not always possible to be able to access the rock faces to collect samples and make measurements. Lichti (2005) used passive RGB colour and intensity data collected with a laser scanner to attempt a maximum likelihood classification of the point cloud into different materials identifiable in the scanned scene. Despite the perceived limitation of the spectral range available, good success rates were reported for natural and man-made targets. The logical next step is to increase the spectral range used, by integrating the lidar data with hyperspectral imagery. The geology application presented here requires the discrimination of more subtle mineral differences than the relatively disparate materials such as buildings and vegetation.

Ground based hyperspectral sensing is a new field, with only a few sensors having been developed in suitable wavelengths for identifying spectral features in common reservoir rocks. For geological applications the advantages of complimenting normal photography with hyperspectral data is the greatly extended spectral range. Many rocks and minerals exhibit characteristic properties at different parts of the spectrum, allowing classification techniques to be applied to identify image regions containing such materials (e.g. van der Meer, 1996). Classification results have the potential to allow a more quantitative approach to analysing the outcrop composition than otherwise available.

3. INSTRUMENTATION

One ground based hyperspectral sensor that has recently been developed is the HySpex SWIR-320m by Norsk Elektro Optikk AS, Norway. This sensor operates in the short wave infra-red (SWIR) part of the electromagnetic spectrum, from 1.3-2.5 µm, giving the required range for detecting absorption bands for common minerals such as carbonates and siliciclastics. Particularly, carbonate minerals are well suited to the SWIR sensor after study by a number of authors (Hunt and Salisbury, 1971; Crowley, 1986; Gaffey, 1986; van der Meer, 1995). The seminal publication by Hunt and Salisbury (1971) presents the spectral curves and absorption features found in carbonate minerals. Gaffey (1986) found at least seven carbonate absorption bands in the 1.6-2.5 µm spectral range due to vibration processes of the carbonate ion, and indicates the position and the shapes of these bands as diagnostic features to identify the rock forming minerals calcite, aragonite and dolomite. Van der Meer (1995) shows that calcite and dolomite form the two end-members of a continuous series with a linear mixture relationship. He concludes that the shape and the exact position of the absorption feature in the 2.3-2.4 µm spectral range may be used to predict the relative abundance of calcite and dolomite in a rock sample. Van der Meer (1996) demonstrates the mapping of carbonate lithofacies from Landsat TM data using spectral mixture models.

Detector	MCT (HgCdTe)
Spectral range	1.3-2.5 µm
Spatial pixels	320
Field of view across track	14º
Pixel field of view	~0.75 mrad
Spectral sampling	5 nm
Spectral bands	256
Digitisation	14 bit

Table 1. Key characteristics of HySpex SWIR-320m sensor

Figure 1 shows the HySpex SWIR-320m sensor in the field. Although it is still a newly developed instrument and not yet fully field "ruggedised", the system is portable enough for field use, and is similar in components to a terrestrial laser scanner, whilst weighing slightly less. The ease of use and portability are critical aspects for geological outcrop work, as field sites are often in remote areas and not always close to roads. With 320 spatial pixels, the hyperspectral sensor is much lower resolution than a contemporary digital camera; however, resolution is sure to increase in the future as it did for CCD/CMOS sensors. For this pilot project, geological problems to be targeted must take into account the scale of features to be studied, as well as the available spatial resolution. The advantage of the HySpex sensor is that is offers high spectral resolution (Table 1). The integration of the hyperspectral data with lidar and visible images therefore allows a complementary approach to obtaining high spatial and spectral coverage of the outcrop.

Figure 1. HySpex SWIR-320m hyperspectral imager.

4. DATA COLLECTION

Because of the suitability of the SWIR sensor for measuring carbonate absorption features, the pilot project for the hyperspectral and lidar integration workflow development was conducted using a carbonate outcrop at Manystones quarry, Peak District, UK. This outcrop, a disused quarry was used to map and quantify dolomitization in Carboniferous Limestone. Transformation of limestone into dolomite is commonly accompanied by an increase in porosity and permeability and provides therefore improved reservoir properties. In the Southern Peak District, shallow marine and reef limestones of the Dinantian period have been affected by

burial dolomitization during the Permian or Triassic periods, and show two stages of dolomitization (Ford, 2002). The second stage contains significant amounts of iron and manganese. No pure dolomite has been found in this area (Ford, 2002). Partly unaltered limestone is found with sharp contact to the dolomite (Figure 2; Figure 3).

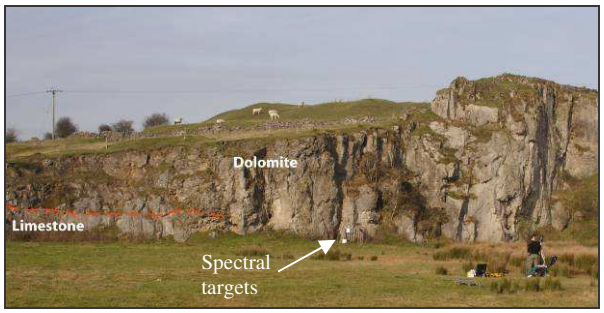

Figure 2. Manystones Quarry, Peak District, UK. The lower section of the outcrop contains unaltered limestone, and the contact with the dolomite is sharp. Outcrop is around 15 m high.

The objectives of the study were:

1. to attempt to automatically map the limestone/dolomite transition;
2. to quantify the amount of limestone/dolomite found in the two areas, and the degree of dolomitization;
3. to establish if limestone existed in the upper part of the outcrop, away from the main limestone bench.

The first of these objectives was deemed to be a basic test of the equipment and data processing workflow, as the limestone bench could be relatively easily identified with a standard visible wavelength image. The second two were more geologically interesting and challenging, as with the naked eye it was not possible to easily identify other areas of limestone within the outcrop, especially in the upper sections that were difficult to access.

Data was collected on a bright, sunny day in November 2007. The HySpex sensor was deployed on a photographic tripod and a number of scans of the outcrop were collected. The distance to the outcrop was approximately 50 m for one set of scans, and 20 m for a second scan position. Because of the field of view of the sensor, more than one scan was required to cover the top and bottom of the outcrop fully. Exposure was chosen to maximise the digital numbers available for the image, with bright features kept just below the over-exposure level. At a single epoch of data collection, the chip samples each spectral band in the spatial line, and a 2D image is built up using a rotation stage, taking around two minutes to capture the whole quarry face. To reduce data noise, scan lines were averaged over ten exposures before the rotation stage was moved.

A Riegl LMS-Z420i terrestrial laser scanner (Riegl, 2008) was also used to capture the geometry of the quarry. A calibrated Nikon D200 camera equipped with a Nikkor 50 mm lens was mounted on top of the scanner and conventional images were exposed to cover the outcrop. These were automatically registered using the known mounting position and orientation relative to the scanner measurement centre. Four scans were acquired to ensure that no shadows (data gaps) were present in the 3D data. Retro-reflective targets were set out on the quarry face and used to register the scans relative to the central scan position.

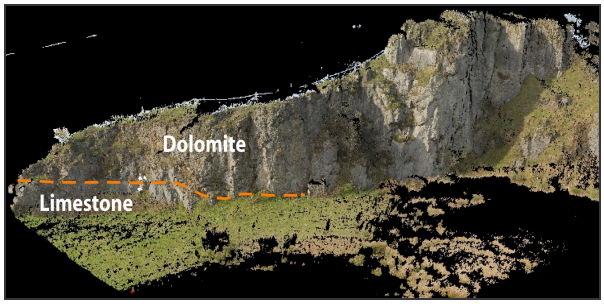

Figure 3. 3D model of Manystones quarry, textured with Nikon camera imagery.

For the spectral data, calibration targets were also set out in the scene, to act as reference spectra during hyperspectral image processing. These targets were made of white and grey linoleum and white paper. Calibration targets with high quality diffusive reflection properties are very expensive and were not available during this work. However, the calibration panels used were corrected relative to a Spectralon diffusive reflector with a reflectance of approximately 99%. This is therefore a cost-effective solution to providing field spectral calibration.

5. PROCESSING WORKFLOW

5.1 Hyperspectral Processing

Hyperspectral images were processed using the Environment for Visualising Images (ENVI) software. Initially the at-sensor radiance was transferred into relative reflectance using the empirical line approach to remove the solar irradiance and the atmospheric path radiance in the image (Figure 5). Reference spectra for the band-wise regressions were provided by the spectral targets positioned on the outcrop during data acquisition. Figure 4 shows the reflectance properties for dolomite and limestone found in the Manystones data.

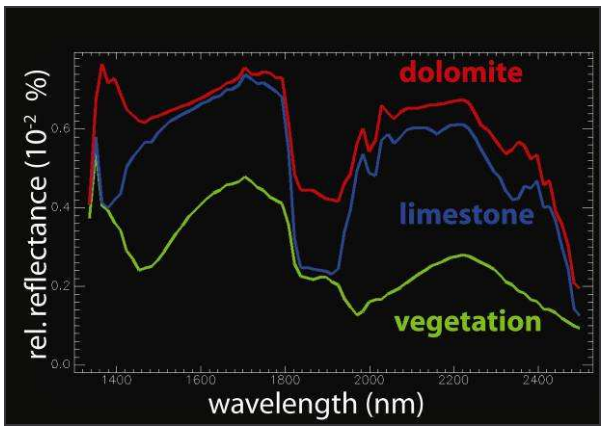

Figure 4. Spectral profile showing reflectance properties for dolomite, limestone and vegetation found in Manystones data.

Figure 5. False colour image (Red: 1720 µm, G: 2009 µm, B: 1563 µm) of Manystones quarry,

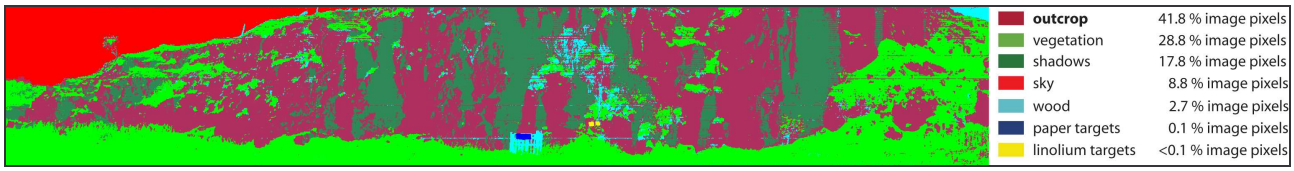

Figure 6. Maximum likelihood classification separating the various areas of the outcrop.

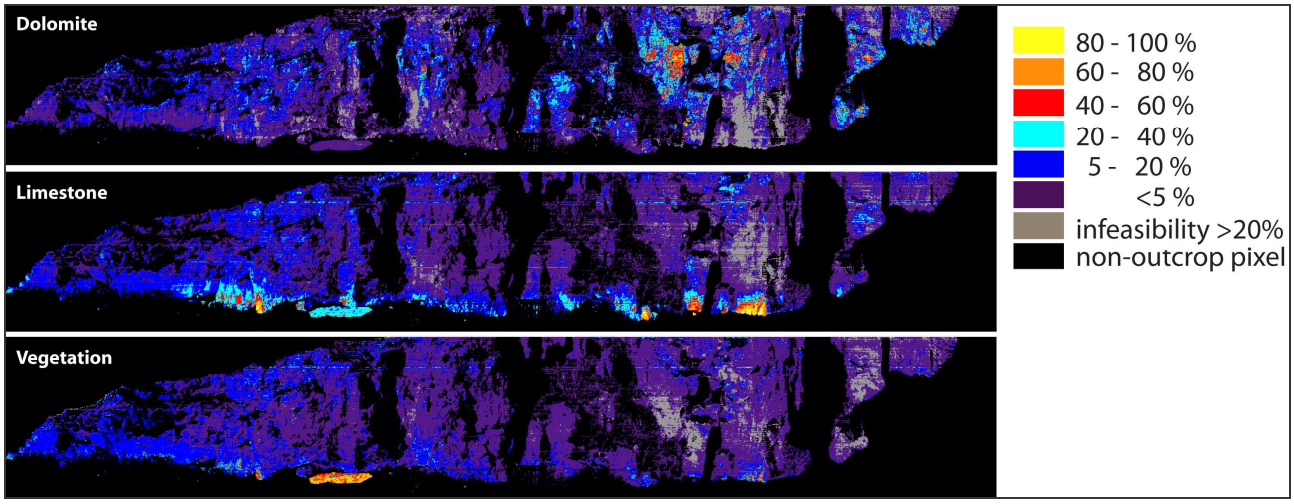

Figure 7. MTMF result for each of the three end members being unmixed, with high infeasibility pixels (grey).

The corrected image was first segregated into geology and non-geology pixels, to eliminate areas of vegetation, man-made materials and spectral/retro-reflective targets. To determine outcrop pixels from non-outcrop pixels a maximum likelihood classifier was applied based on the first ten bands of a minimum noise fraction (MNF) transform (Boardman and Kruse, 1994), a transformation examining the principal components to determine the image dimensionality and remove noise (Figure 6). Some areas of the outcrop were affected by shadows caused by rock corners and the sun angle during data collection. These areas were characterised by a very low signal to noise ratio. Therefore, shadowed areas were erroneously classified as non-geology pixels. The MNF transform was applied to the reflectance values of the outcrop pixels, removing bands with low eigenvalues (<5) and those with approximately equal eigenvalues. The most coherent bands of the MNF transform were retained with noise removed. During this stage of processing, it was apparent that a significant amount of noise occurred in the image data. On closer inspection, this was attributable to a higher than expected number of dead pixels on the chip, resulting in lines of interpolated data across the image bands (visible in Figures 6 and 7). Some corrections to the electronics have since been made by the producer of the sensor.

Based on the first ten MNF bands, end-members of the different pure materials were collected using pure-pixel indices. Dolomite, limestone and vegetation could be identified as spectrally unique. Although it was expected that clay minerals should be found in the image, an end-member relating to clay was not identified in this stage of processing, perhaps due to the image noise or insufficient reflectance correction. The final stage of hyperspectral processing was to classify the dataset using the end-members identified. The Mixture Tuned Matched Filtering (MTMF) approach (Boardman, 1998) was applied to spectrally unmix the outcrop pixels, giving each pixel a score corresponding to the similarity with the end-members. One such image was produced for each end-member defined (Figure 7). Infeasibility values were in some cases high, again related to the dead pixels in the image that were kept during processing, as well as small areas in direct sunlight that had been over-exposed.

5.2 Lidar Processing

The raw scan data were registered using the control targets located between the scans. A triangulation of a single scan was performed and textured with the digital imagery collected simultaneously with the 3D data. The photorealistic model was used to visualise the outcrop surface and provided

a partial check of results of hyperspectral processing, as well as being a background for geological interpretation.

5.3 Data Fusion

The hyperspectral imagery and classifications alone provide only qualitative data that can be interpreted by the geologist. For a quantitative assessment, it is necessary to register the hyperspectral imagery to a real-world coordinate system, so that classified pixels can be located in the object space and spatially interrogated. Because the HySpex sensor operates on a linear scan array basis, it is not possible to process the imagery photogrammetrically using the central perspective projection. The result of scanning is a panoramic image representing a cylindrical projection, requiring an alternative geometric model to be applied. The geometric model for panoramic cameras has been presented by Schneider and Maas (2006) with extension for additional parameters for modelling the internal geometry of the sensor. Application of the model in space resection, calibration and combined bundle adjustment with central perspective images has validated this model.

The panoramic model of Schneider and Maas (2006) was applied to the HySpex imagery. To establish the correspondence of the HySpex data with the lidar coordinate system, control points were measured in the imagery. The ten retro-reflective targets and corners of the spectral targets provided easily identifiable points, which were supplemented with natural control points distributed over the remainder of the imagery. Initially, space resection was performed to obtain the camera position and orientation for each panoramic image, with favourable results. As a second step, four images representing the top and bottom of the outcrop from two scan positions were combined with the conventional imagery acquired from on top of the laser scanner in a bundle adjustment. This enabled the positions and orientations of the imagery, as well as the calibration parameters to be recovered.

With the hyperspectral images registered to the lidar coordinate system, it was possible to relate the image data to the actual outcrop geometry to perform more quantitative analysis, as well as visualisation. Because the classified images from hyperspectral processing are kept at the same dimensions as the raw image data, it is possible to use the same calibration and orientation parameters for these results as well. As an initial test of this, the classified images were used to colour the lidar point cloud, resulting in a highly visual result of the classification when displayed together with the virtual outcrop model created in Section 5.2. Each point in the point cloud was projected into the classified image and the colour value assigned. The coloured points were then filtered to keep only points relating to the dolomite and limestone rock types, so that weak results from the MTMF, non-classified and vegetation points were removed, leaving only the stronger signals. Results were then combined to create a visualisation superimposing the coloured classified data points onto the textured model (Figure 8).

6. RESULTS

The classification shows the spatial distribution of limestone and dolomite within the outcrop. Initial field observations suggested that the lower part of the outcrop was limestone and the upper portion was dolomitized. The hyper-spectral image illustrates that the situation is far more complex and the alteration of the upper portion to dolomite is not uniform and is incomplete. Residual patches of limestone prevail and the spectral data illustrate that the degree of dolomitization varies. From this image it is possible to extract quantitative data on the spatial distribution of the dolomitization which was not previously attainable. Variations in dolomitization are interpreted to result from differences in diagenetic fluid pathways.

7. CONCLUSION

This paper has demonstrated the application of a ground based hyperspectral sensor for the study of geological outcrops. The use of such a sensor has the benefits of being able to distinguish the spatial distribution of different rock types, in a non-contact manner, and with a higher spectral resolution than possible with conventional camera imagery. The results of this preliminary study are highly promising, having identified the distribution of limestone in a dolomitized quarry with greater resolution than possible with disparate field samples. Integration of the hyperspectral imagery with detailed lidar geometry, using the panoramic camera model, allows the classification results to be projected into 3D space to make more quantitative analysis.

Problems with the sensor electronics during this first test resulted in more noise than expected, and difficulties with reflectance correction remain to be solved, as models for conventional airborne data are not applicable. Further work will investigate this aspect further, as well as try more classification methods, and develop a texturing routine for the classified images. There is also much assessment to be carried out to validate the classified areas and the success of processing results, as well as gain more quantitative measures from the data.

Integration of hyperspectral and lidar data provides the geologist with novel methods for gaining meaningful outcrop data, with much higher spatial resolution than previously possible.

ACKNOWLEDGEMENTS

This project is funded by the Norwegian Research Council and StatoilHydro ASA through the Petromaks program. Thanks to Ivar Baarstad and Trond Løke from Norsk Elektro Optikk AS for technical support and instruction in scanner handling. Thanks to Peter Gutteridge for acting as a field guide for the dolomite outcrops in the Peak District.

REFERENCES

Bellian, J.A., Kerans, C. and Jennette, D.C., 2005. Digital outcrop models: applications of terrestrial scanning lidar technology in stratigraphic modeling. *Journal of Sedimentary Research*, 75(2), pp. 166-176.

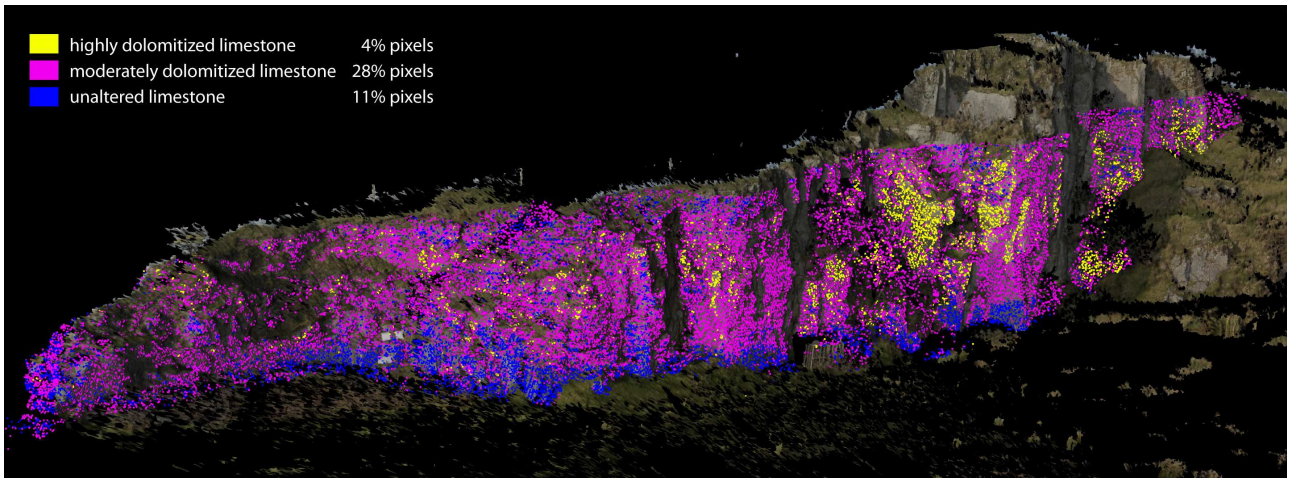

Figure 8. Classified point cloud superimposed with textured lidar model of Manystones quarry.

Boardman, J.W., 1998. Leveraging the high dimensionality of AVIRIS data for improved sub-pixel target unmixing and rejection of false positives: Mixture tuned matched filtering. In: *Summaries of the Seventh Annual JPL Airborne Geoscience Workshop, Pasadena, CA*.

Boardman, J.W. and Kruse, F.A., 1994. Automated spectral analysis: A geological example using AVIRIS data, northern Grapevine Mountains, Nevada. In: *Proceedings, Tenth Thematic Conference, Geologic Remote Sensing*, 9-12 May 1994, San Antonio, Texas, pp. I407-I418.

Bowen, B.B., Martini, B.A., Chan, M.A. and Parry, W.T., 2007. Reflectance spectroscopic mapping of diagenetic heterogeneities and fluid-flow pathways in the Jurassic Navajo Sandstone. *AAPG Bulletin*, 91(2), pp. 173-190

Buckley, S.J., Howell, J.A., Enge, H.D., Leren, B.L.S. and Kurz, T.H., 2006. Integration of terrestrial laser scanning, digital photogrammetry and geostatistical methods for high-resolution modelling of geological outcrops. In: *The International Archives of the Photogrammetry, Remote Sensing and Spatial Information Sciences*. Dresden, Germany, Vol. XXXVI, Part B5, proceedings CD.

Buckley, S.J., Howell, J.A., Enge, H.D. and Kurz, T.H., 2008. Terrestrial laser scanning in geology: data acquisition, processing and accuracy considerations. *Journal of the Geological Society, London*, 165(3), pp. 625-638.

Crowley, J.K., 1986. Visible and near-infrared spectra of carbonate rocks: reflectance variations related to petrographic texture and impurities. *Journal of Geophysical Research*, 91(B5), pp. 5001-5012.

Enge, H.D., Buckley, S.J., Rotevatn, A. and Howell, J.A. 2007. From outcrop to reservoir simulation model: workflow and procedures. *Geosphere*, 3(6), pp. 469-490.

Ford, T.D., 2002. Dolomitization of the Carboniferous Limestone of the Peak District: a review. *Mercian Geologist*, 15(3), pp. 163-170.

Gaffey, S.J., 1986. Spectral reflectance of carbonate minerals in the visible and near infrared (0.35-2.55 microns): calcite, aragonite, and dolomite. *American Mineralogist*, 71, 151-162.

Hunt, G.R. and Salisbury, J.W., 1971. Visible and near-infrared spectra of minerals and rocks: II. carbonates. *Modern Geology*, 2, pp. 23-30.

Lichti, D.D., 2005. Spectral filtering and classification of terrestrial laser scanner point clouds. *The Photogrammetric Record*, 20(111), pp. 218-240.

McCaffrey, K.J.W. et al., 2005. Unlocking the spatial dimension: digital technologies and the future of geoscience fieldwork. *Journal of the Geological Society, London*, 162(6), pp. 927-938.

Riegl, 2008. Terrestrial scanner overview, http://www.riegl.com/terrestrial_scanners/terrestrial_scanner_overview/terr_scanner_menu_all.htm (accessed 27 April, 2008).

Sagy, A., Brodsky, E.E. and Axen, G.J., 2007. Evolution of fault-surface roughness with slip. *Geology*, 35(3), pp. 283-286.

Schneider, D. and Maas, H.-G., 2006. A geometric model for linear-array-based terrestrial panoramic cameras. *The Photogrammetric Record,* 21(115), pp. 198-210.

Van der Meer, F., 1995. Spectral reflectance of carbonate mineral mixtures and bidirectional reflectance theory: quantitative analysis techniques for application in remote sensing. *Remote Sensing Reviews*, 13(1-2), pp. 67-94.

Van der Meer, F., 1996. Spectral mixture modelling and spectral stratigraphy in carbonate lithofacies mapping. *ISPRS Journal of Photogrammetry and Remote Sensing*, 51(3), pp. 150-162.

Windeler, D.S. and Lyon, R.J.P., 1991. Discriminating dolomitization of marble in the Ludwig Skarn near Yerington, Nevada using high-resolution airborne infrared imagery. *Photogrammetric Engineering and Remote Sensing*, 57(9), 1171-1177.